UHASSELT

KNOWLEDGE IN ACTION

Maastricht University

Faculty of Medicine and Life Sciences
School for Life Sciences

Master of Biomedical Sciences

Master's thesis

Microglial branch motility and morphology are regulated by TRPV4 channel

Melanie Mertens
Thesis presented in fulfillment of the requirements for the degree of Master of Biomedical Sciences, specialization Molecular Mechanisms in Health and Disease

SUPERVISOR :
Prof. dr. Bert BRONE

CO-SUPERVISOR :
dr. Yeranddy AGUIAR ALPIZAR

MENTOR :
Mevrouw Jolien BEEKEN

Transnational University Limburg is a unique collaboration of two universities in two countries: the University of Hasselt and Maastricht University.

UHASSELT
KNOWLEDGE IN ACTION

**2020
2021**

Faculty of Medicine and Life Sciences
School for Life Sciences

Master of Biomedical Sciences

Master's thesis

Microglial branch motility and morphology are regulated by TRPV4 channel

Melanie Mertens
Thesis presented in fulfillment of the requirements for the degree of Master of Biomedical Sciences, specialization Molecular Mechanisms in Health and Disease

SUPERVISOR :
Prof. dr. Bert BRONE

CO-SUPERVISOR :
dr. Yeranddy AGUIAR ALPIZAR

MENTOR :
Mevrouw Jolien BEEKEN

Microglial branch motility and morphology are regulated by TRPV4 channel*

Melanie Mertens[1], Jolien Beeken[2,3], Bert Brône[2] and Yeranddy A. Alpizar[2]

[1]Biomedical Sciences, Faculty of Medicine and Life Sciences, Hasselt University, Campus Diepenbeek, Agoralaan building D - B-3590 Diepenbeek, Belgium
[2]Neuroscience research group, Biomedical Research Institute, Hasselt University, Campus Diepenbeek, Agoralaan building C - B-3590 Diepenbeek, Belgium
[3]Molecular Regulation of Neurogenesis, GIGA-Stem cells, University de Liège, Quartier Hôpital, avenue Hippocrate 15, 4000 Liège, Belgium

*Running title: *TRPV4 channel in microglial functions*

To whom correspondence should be addressed: Bert Brône, Tel: +32 (11) 26 92 37; Email: bert.brone@uhasselt.be

Keywords: TRPV4, microglia, branch motility, morphology, phagocytosis

ABSTRACT

Microglial branch dynamics are crucial for surveillance of the brain and directed motility towards injured regions to maintain homeostasis. By extending and retracting their processes via Ca^{2+}-dependent cytoskeletal rearrangements, microglia perceive signals from their environment. Chemical cues are major stimuli for branch motility by inducing acute changes in intracellular Ca^{2+}, driven by purinergic receptors. Next to chemical signals, microglia receive mechanical forces from the extracellular matrix, implying the involvement of other Ca^{2+}-dependent pathways. In this project, we investigate the role of the mechanosensitive Ca^{2+} channel TRPV4 (Transient Receptor Potential vanilloid 4) in the motile response of microglia. We prepared fixed and acute brain slices showing eGFP-expressing microglia and isolated microglial cells to study density, morphology, (directed) process motility and phagocytosis in the mouse cortex after genetic ablation or pharmacological inhibition of TRPV4. Using confocal microscopy on fixed brain slices, we demonstrated that microglia are homogeneously distributed throughout the brain in the absence of TRPV4. However, *Trpv4*-deficient microglia exhibit a decrease in total process length and the number of tips and branch points, showing an overall reduction in morphological complexity. Besides, time-lapse two-photon microscopy of acute cortical slices revealed that in the absence or inhibition of TRPV4 microglial processes survey less brain area. In contrast, after applying a laser-induced brain injury, *Trpv4* deficiency does not alter process extension towards the lesion. Lastly, cultured microglia lacking TRPV4 showed a lower phagocytic uptake of synaptosomes. These findings imply the role of TRPV4 in the process of microglial motility, morphology and phagocytosis.

INTRODUCTION

Microglia are the primary immune cells of the central nervous system (CNS) and play an essential role in maintaining normal brain function (1, 2). They are derived from primitive yolk sac progenitors that arise during embryogenesis. Early in development, microglia invade the brain and transform into highly ramified phagocytes that regulate brain development and cognitive function (1-3). They drive neurogenesis, synaptogenesis and neuronal activity, eliminate redundant neurons and connections and strengthen synaptic connections selectively (1, 2).

By self-renewal of their cell population, microglia are maintained after birth and into adulthood, where they remain essential to control brain homeostasis (4, 5). The cells mediate inflammatory reactions by interacting with other infiltrating immune cells, maintain neuronal

networks, stimulate tissue and injury repair and eliminate microbes, dead and damaged cells and redundant synapses via phagocytosis (1, 4, 6). Given the high importance of microglia during development and throughout life, microglial dysfunction is implicated in several neuropsychiatric disorders such as schizophrenia, autism spectrum disorder and epilepsy, which strongly affect life quality (3, 7-9).

In the healthy brain, microglia have small somas and a highly branched morphology with long processes and fine termini (10, 11). The cells are extremely motile and constantly change their morphology, for which they rely on the motility and dynamics of their processes. It allows them to carry out their functions and control brain homeostasis (12, 13). Microglia actively extend and retract their processes to survey the brain in response to neuronal activity and changes in the microenvironment. This way, they can adapt to their environment and communicate with surrounding cells (8, 14-18). Brain surveillance occurs over intervals of seconds to minutes, with branches extending up to several micrometers or retracting entirely without changing the total number of processes (10). Several factors contribute to the process, such as microglial density, the number of processes, process length and ramifications and speed and frequency of process extensions and retractions (12). Therefore, the morphological characteristics of the cells determine the degree of motility.

Microglia express a wide array of membrane receptors on their processes, which allow them to sense a myriad of pathologic events or changes in brain homeostasis during surveillance (1, 14, 17). These evoke microglial activation and motility of microglial processes towards the damaged region without cell body movement (6, 10, 16, 19). The cells already respond within the first minute after injury by extending their processes close to the lesion after process tips appear bulbous and enlarged a bit (10). After 30 min, branches of surrounding cells reach the lesion and retract their processes that were directed the opposite way (10, 18). Even more distant cells are attracted and respond by showing directed motility towards the injury without reaching the site (10). After the rapid response of individual microglial processes, the cells retract their processes. They become less

ramified, with fewer, shorter processes and larger somas allowing phagocytosis of harmful components to restore homeostasis (11, 14, 20, 21).

Microglial branch motility, morphology and phagocytosis are dependent on intracellular Ca^{2+} concentrations ($_i[Ca^{2+}]$) (18, 22, 23). *In vivo* studies showed that resting microglia display Ca^{2+} signaling in their processes without significant fluctuations in somatic Ca^{2+} levels (16, 18, 22). Signals from the extracellular environment, such as neuronal activity, trigger microglial Ca^{2+} activity in the processes and control microglial surveillance (18). On the other hand, non-homeostatic brain conditions trigger microglial activation, which is also associated with Ca^{2+} signaling, mainly evoked in the processes. This is correlated with process motility, more specifically, process outgrowth or extension towards the stimuli followed by phagocytic activity. The increase of $_i[Ca^{2+}]$ is evoked by the release from intracellular stores or entry through ligand-gated and/or store-operated Ca^{2+} channels. This triggers the rearrangement of the actin cytoskeleton by stimulating the turnover of actin filaments which results in brain surveillance or microglial activation depending on the size of the environmental stimulus (12, 13, 23).

Chemical cues such as adenosine triphosphate (ATP) released from astrocytes or damaged sites are major triggers for microglial surveillance and directed motility (10, 11, 14, 18). ATP is one of the most important agonists of microglial Ca^{2+} signaling. It is detected by the cell's chemosensors, such as metabotropic and ionotropic purinergic receptors, which increase $_i[Ca^{2+}]$ thereby stimulating cytoskeletal dynamism, hence branch motility (10, 11, 13, 14, 18, 23).

Microglia strongly interact with the extracellular matrix (ECM) (3). Next to chemical stimuli, the cells continuously receive physical signals via remodeling of the ECM (3). Mechanosensation is a crucial cellular process regulating several functions (24). In microglia, mechanical forces are sensed by ß1 integrin receptors, which form a dynamic interface between the ECM and the actin cytoskeleton, providing motility (3, 25). However, integrin responses proceed slowly, indicating the contribution of fast Ca^{2+}-dependent mechanosensation pathways (26).

Next to purinergic receptors, the involvement of non-selective cation channels like Transient

2

Receptor Potential (TRP) channels in microglial motility has been suggested (3, 21, 27). The TRP superfamily consists of six subtypes which are all tetramers with six putative transmembrane domains and sensitive to mechanical, thermal or chemical stimuli (27, 28). TRP channels are widely expressed in neuronal and non-neuronal tissues, where they are essential for regulating $_i[Ca^{2+}]$ and involved in several cellular processes such as proliferation, activation and cell death (27, 29). Microglia have been shown to express several TRP subtypes, including TRPM, TRPC and TRPV (27). TRP melastatin subtype 2 (TRPM2) regulates Ca^{2+}-dependent microglial activity in response to stress and reactive oxygen species (27, 30). TRPM4 is a Na^+ channel that is sensitive to $_i[Ca^{2+}]$ and is likely implicated in membrane depolarization via exocytosis-related processes (27, 31). TRPM7 contributes to microglial migration and possibly other Ca^{2+}-induced functions in response to tyrosine phosphorylation (27, 29). Besides, TRP canonical subtypes 1 and 3 (TRPC1, 3) are suggested to mediate immune responses in microglia in a Ca^{2+}-regulated way (27). Next, TRP vanilloid subtype 1 (TRPV1) is a thermoreceptor mainly expressed on intracellular organelles such as mitochondria, endoplasmic reticulum (ER) and Golgi with little expression on the plasma membrane. The channel plays a vital role in microglial migration by increasing intramitochondrial Ca^{2+} concentrations (27, 32). TRPV2 is a thermo- and mechanoreceptor and is known to involve in microglial phagocytosis (27, 33). Lastly, TRPV4 has been suggested to regulate microglial activity through the channel's mechanosensitive properties (21, 27). However, which of these channels might contribute to an increase in $_i[Ca^{2+}]$ and thereby induce cytoskeletal rearrangements to provide microglial process motility is not known yet.

As described above, TRPV4 is a mechanosensitive channel expressed in microglia and is involved in many different cellular functions (27, 34-36). Besides microglia, the channel is expressed in several tissues like the lung, skin, endothelium, chondrocytes, astrocytes, sensory neurons and neurons of the CNS (21, 27, 34, 37). TRPV4 oligomerizes in the ER via its C-terminus and translocates to the plasma membrane (38). It is a Ca^{2+}- and Mg^{2+}-permeable channel, and therefore, channel activation induces the influx of Ca^{2+} (39,

40). Several endogenous stimuli are direct activators of TRPV4, such as changes in osmolarity, mechanical stress, cell swelling, stretch, shear flow, temperature changes and low pH (35, 37, 41).

In neurons, TRPV4 functionally interacts with tubulin, actin and neurofilament proteins via its C-terminus in a mutual way (42). Goswami *et al.* demonstrated colocalization of the receptor with actin-rich structures like filopodia, lamellipodia and focal adhesion points. This way, TRPV4 regulates the morphology and determines the net movement of neurites by steering growth cone movements. On the other hand, the cytoskeleton regulates Ca^{2+} influx through TRPV4 as described for endothelial cells (26, 42). In astrocytes, TRPV4 influences the intracellular pathways in the astrocytic endfeet (37).

The role of TRPV4 in microglia has not been extensively studied. Konno *et al.* showed that in response to lipopolysaccharides, an outward Ca^{2+} current is evoked, suppressing microglial activation (21, 37). On the other hand, mechanical stimulation increases microglial TRPV4 expression and cellular activity (37, 43). The involvement of TRPV4 in the regulation of Ca^{2+}-induced cytoskeletal dynamics and cell motility and morphology strongly suggests its role in microglial motility. In this project, we explore the contribution of TRPV4 channel activity in the control of branch motility, morphology and phagocytosis in microglia of the cerebral cortex. This is possible by investigating whether these microglial features are decreased in the absence of the Ca^{2+} channel. We hypothesize that the lack or inhibition of TRPV4 channels decreases microglial branch organization, motility and phagocytic activity.

The effect of TRPV4 ablation on microglial density is first analyzed to provide an overview of the cellular distribution within the cortex. Likewise, we measure microglial density within the hippocampus, which is higher than density in the cortex (44). The hippocampus will be more elaborated and studied during the next project. We first focus on the cerebral cortex since this region is easily accessible and provides nicely dispersed and ramified microglia, hence ideal for characterizing the cells. We will characterize microglial morphology in a *Trpv4*-deficient model since next to branch motility, it is strongly dependent on

3

cytoskeletal dynamics (13). In addition to density and morphology, we investigate microglial surveillance, directed motility and phagocytosis after genetic ablation or acute inhibition of TRPV4. More insight into these processes is necessary to better understand the complexity of microglial functioning during homeostatic and non-homeostatic conditions.

EXPERIMENTAL PROCEDURES

Animals - $CX_3CR_1{}^{eGFP/-}Trpv4^{-/-}$ (referred to as *Trpv4* knockout (KO)) and $CX_3CR_1{}^{eGFP/-}Trpv4^{+/+}$ (referred to as wild type (WT)) littermate C57BL/6 mice were used for all experiments (eGFP, enhanced green fluorescent protein). Animals were obtained by in-house breeding, as described in Fig. 1A. Mice were housed on a 12 h light/dark cycle in a standard animal care facility, with access to food and water *ad libitum*. Housing and experiments were conducted following the guidelines of the Belgian Law and the European Council Directive and with the approval of the Ethical Committee on Animal Research of Hasselt University.

Genotyping - Newborns were genotyped for *Trpv4* and *CX₃CR₁*-eGFP at postnatal day 7-12 (P7-12) using PCR technology. DNA from toe biopsies was extracted using 10x Kapa Express extraction buffer, 1 U/µl Kapa Express extraction enzyme (KAPA Biosystems, USA) and Milli-Q water. DNA samples were diluted in a PCR mix solution containing 10 µM of each primer for *Trpv4* or *CX₃CR₁* (Table 1) in Kapa2G Fast genotyping mix.

Table 1 - Primer sequences for *Trpv4* and *CX₃CR₁*

Gene	Forward	Reverse
Trpv4	5'CATGAAATCT GACCTCTTGTC CCC3' 5'CTGTCCCAGC CTCCCCTCCT3'	5'GCTCCTGTTG AACATGCTTAT CG3'
CX₃CR₁	5'CTCCCCCTGA ACCTGAAAC3' 5'GTCTTCACGT TCGGTCTGGT3'	5'CCCAGACAC TCGTGTCCTT3'

The following PCR program was run: 1x 3 min at 95 °C; 40x 15 sec at 95 °C + 15 sec at 65 °C + 1 min at 72 °C; 1x 1 min at 72 °C and kept at 4 °C. The samples were loaded on a 3% agarose gel (UltraPure Agarose (Invitrogen, USA), TAE 1x, 1:10000 GelRed (Biotium, USA)) together with a 200-10 000 bp DNA SmartLadder (Eurogentec, Belgium) as a control, and migration was launched at 145 V. Gels were read using D-Digit (LI-COR Biosciences, Germany). WT and *Trpv4* KO animals were used for experiments, and mice with other genotypes were discarded based on the outcome.

Fixed brain slice preparation - P21 mice were anesthetized with an intraperitoneal injection of 40 mg/ml Dolethal (Vetoquinol, Belgium) and transcardially perfused with phosphate-buffered saline (PBS) containing 20 units of heparin (LEO Pharma, Belgium) followed by 4% paraformaldehyde (PFA). Brains were dissected and fixed for 24 h in 4% PFA, then washed three times with PBS and stored on PBS-azide (0.1%). Next, coronal sections (100 µm) were cut using an HM650 V microtome (Thermo Fisher Scientific, USA). Brain sections were then incubated for 15 min with 4,6-diamidino-2-phenylindole (DAPI, Sigma-Aldrich, Belgium), washed with PBS and Milli-Q water and mounted on glass slides using Immu-Mount mounting medium (Thermo Fisher Scientific). These slices were used to study microglial distribution and morphology.

Fluorescence microscopy - Cortical brain sections were imaged using an automated slide scanner (AxioScan.Z1, Zeiss, Germany). Microglial density was quantified in secondary motor area layers 1, 2/3 and 5 of the cortex by calculating the number of cells per area (mm^2) for each layer. The volumetric density of microglia in the cortex was studied by imaging the slices using a Zeiss LSM880 confocal microscope with a 63x oil immersion objective (NA 1.4). Cells labeled with eGFP were imaged at a wavelength of 488 nm with a pixel dwell time of 4.10 µs, a frame size of 1024x1024 pixels and a depth of 20 µm. Cells were counted using Fiji (45) and divided by the volume of the total image.

Microglial morphology was assessed by Sholl analysis, using confocal images obtained as described above. Cells were cropped out in 2D in Fiji and reconstructed using 3D automatic cell tracing in Vaa3D software (46), which uses the

4

APP2 (all-path-pruning 2.0) algorithm to reconstruct ramified cells in 3D. A data file was provided with all information, and morphological parameters were extracted using custom code written in MATLAB (MathWorks, USA).

Cortical brain slices for ex vivo imaging - P21 mice were decapitated and brains dissected on an ice-cold standard slicing solution containing (in mM) 120 N-methyl-D-Glucamine, 2.4 Sodium Pyruvate, 1.3 Sodium-L-Ascorbate, 7 $MgCl_2$ (Sigma-Aldrich), 2.5 KCl, 1 $CaCl_2$, 1.2 NaH_2PO_4, 20 D-Glucose (VWR International, USA), 25 $NaHCO_3$ (Alfa Aesar, USA), bubbled with 95% O_2/5% CO_2, pH 7.4. Acute coronal sections (300 µm) were obtained using a VT1200S vibratome (Leica Biosystems, Germany). Brain sections were transferred to artificial cerebrospinal fluid (aCSF; (mM) 126 NaCl (VWR International), 2.5 KCl, 26 $NaHCO_3$, 1.25 NaH_2PO_4, 10 D-Glucose, 2 $MgCl_2$, 2 $CaCl_2$, pH 7.4) and allowed to recover for 1 h at 37 °C. A selected group of slices derived from WT mice was incubated in aCSF containing 10 µM of a specific blocker of TRPV4 (GSK2193874 (GSK21), Tocris Bioscience, UK). After that, one cortical slice was transferred within aCSF to an O_2-supplied 35 mm Petri dish for imaging.

Two-photon microscopy - Acute cortical slices were imaged in an LSM880 with a 40x water objective (NA 1.1) and a Mai Tai DeepSee eHP Ti:Sapphire infrared laser (Spectra-Physics, Belgium) at 920 nm. To avoid measuring activated microglia because of the slicing procedure, the working focal section was defined at least 50 µm above the glass bottom. Selected regions were imaged for ten cycles with an interval of 1 min, at a pixel dwell time of 1.54 µs, a frame size of 512x512 pixels and a depth of 15 µm using the laser power at 13.2 mW. Microglial surveillance was quantified in 2D maximum intensity projections using Fiji. First, the background was subtracted (radius 30 pixels) followed by a median filter of 1 pixel. Drifting during imaging was corrected (StackReg plugin), cells were cropped and thresholded. The newly surveyed brain area was quantified by subtracting image at time t+1 from the image at time t for each cell individually.

Directed motility of microglial processes was evoked by illuminating a 5x5 µm area of the cortex for 1 min using the Mai Tai DeepSee Ti:Sapphire laser at 110 mW laser power. After applying the laser-induced lesion, brain sections were imaged for 15 cycles with an interval of 1 min between each cycle, as described above. Images were converted to 2D and analyzed using Fiji to quantify process motility towards the laser-induced brain injury. Drifting was corrected, a median filter was applied and background subtracted as previously described. Quantification of the average process speed per cell was done by manually tracking bulbous tips extending towards the lesion as long as they kept moving.

Phagocytosis of synaptosomes - P21 WT and *Trpv4* KO littermate pups were euthanized and whole brains dissected and homogenized as previously described (47). Meninges were removed, and after homogenization, the resulting single-cell suspension was selected for CD11b^{+} (monocyte marker) cells via magnetic bead separation (Miltenyi Biotec, Germany). CD11b^{+} microglia were seeded on Poly-D-Lysine (Gibco, USA) and Collagen IV (Sigma-Aldrich) pre-coated coverslips in 24-well plates in serum-free medium (DMEM/F12, Gibco) for seven days at 37 °C and 10% CO_2, supplemented with: (from Sigma-Aldrich unless stated otherwise) 1% penicillin-streptomycin (Gibco), 5 µg/ml insulin, 5 µg/ml N-Acetyl-Cysteine, 100 µg/ml apo-transferrin, 100 ng/ml Na^+-Selenite, 1 µg/ml heparan sulfate, 2 µg/ml human TGFß-2 (PeproTech, USA), 100 ng/ml murine IL-34, 1.5 µg/ml cholesterol and 2 mM glutamine (Gibco). After ten days, cells were incubated with DMEM/F12 containing Dil-labeled synaptosomes for 1 h. Synaptosomes were isolated from adult mice and stained with 1,1′-dioctadecyl-3,3,3′,3′-tetramethylindocarbocyanine perchlorate (Dil) using Syn-PER™ Synaptic Protein Extraction Reagent (Thermo Scientific). When indicated, WT cells were also incubated with GSK21 (1 and 10 µM). Coverslips were then mounted with a DAPI-containing mounting medium (Vectashield). The LSM880 was used to image the cells at 20x (NA 0.8) and wavelengths of 488 and 543 nm were used to visualize eGFP and Dil-labelled synaptosomes. DAPI-containing nuclei were visualized using the two-photon laser at 810 nm. Images were acquired with a pixel dwell time of 4.10 µs and a frame size of 512x512 pixels. The average synaptosome uptake per cell was quantified in Fiji by cropping out the cells and measuring the cargo of synaptosomes inside the cell.

Statistical analysis - Statistical analysis was performed using Prism9 (GraphPad Software, USA). Two means were compared using the unpaired, two-tailed Mann-Whitney U test. The Kruskal-Wallis, followed by Dunn's multiple comparison test, was used to compare multiple groups. Multiple single comparisons were performed using unpaired, multiple Mann-Whitney U test. Two categorical groups were checked using Fisher's exact test, and the Chi-square test was performed to compare observed data with expected values. The normality of data was checked using the Kolmogorov-Smirnov test. Differences with p values < 0.05 are considered significant.

RESULTS

Developmental differences between WT and Trpv4 KO littermates - To study the involvement of the mechanosensitive TRPV4 channel in microglial motility, morphology and phagocytosis, we characterized *Trpv4*-deficient microglia in the cortex. For this purpose, we started two breedings as described in Fig. 1A to obtain WT and *Trpv4* KO littermates. We first investigated the effect of genetic ablation of *Trpv4* on development by checking whether both breeding strategies follow the Mendelian distribution of 25:50:25, regardless of their CX_3CR_1 genotype (Fig. 1B). A total of 189 mice was obtained from the $CX_3CR_1^{eGFP/-}Trpv4^{+/-}$ x $CX_3CR_1^{eGFP/-}Trpv4^{+/-}$ breeding with 47 WT, 94 heterozygous and 48 *Trpv4* KO mice. From the $CX_3CR_1^{eGFP/eGFP}Trpv4^{+/-}$ x $CX_3CR_1^{-/-}Trpv4^{+/-}$ breeding, 58 WT, 148 heterozygous and 51 *Trpv4* KO mice were obtained. By comparing the observed distribution with the expected Mendelian 25:50:25 ratio, we found that only breeding 1 is significantly distributed according to this ratio. However, Fisher's exact test shows no significant difference between the total number of WT and *Trpv4* KO mice 21 days after the birth of both breedings. This indicates that both genotypes develop equally, and therefore, a *Trpv4* deficiency does not affect embryonic and postnatal development. Next to survival, we compared the total body weight of WT and *Trpv4* KO littermates to investigate the phenotype of the *Trpv4* KO animals (Fig. 1C). At P21, WT animals have a weight that varies between 7-11 g. *Trpv4* KO littermates have no significantly lower weight showing that a TRPV4 receptor KO is not associated with a lower weight of the animals at P21.
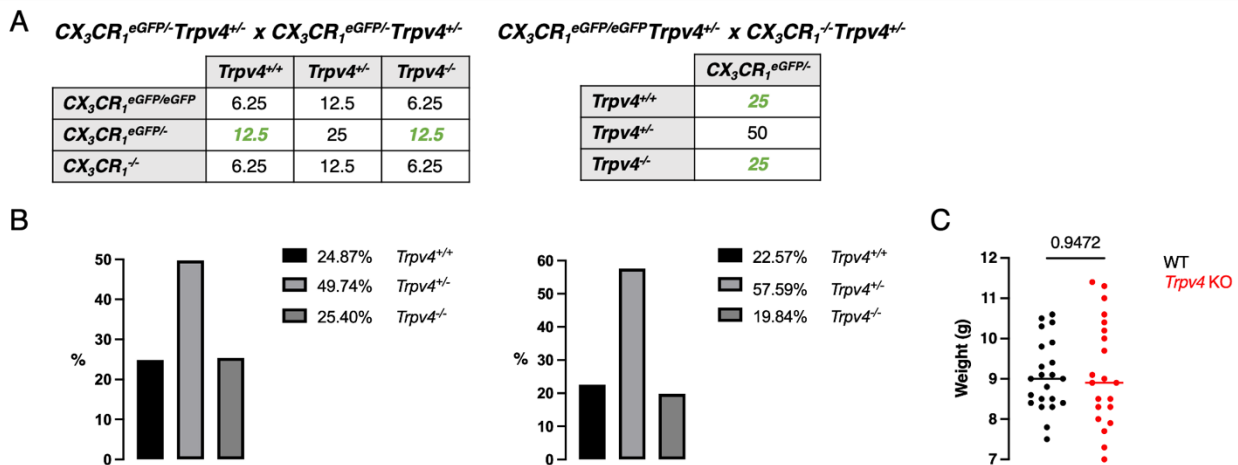

Fig. 1 - Breeding strategy and development of *Trpv4*-manipulated litters. (A) Overview of the Mendelian distribution of breeding 1 ($CX_3CR_1^{eGFP/-}Trpv4^{+/-}$ x $CX_3CR_1^{eGFP/-}Trpv4^{+/-}$) and breeding 2 ($CX_3CR_1^{eGFP/eGFP}Trpv4^{+/-}$ x $CX_3CR_1^{-/-}Trpv4^{+/-}$), respectively. The green values indicate the genotypes that were used for experiments. **(B)** Distribution of the *Trpv4* genotypes of the mouse pups of both breedings, regardless of their CX_3CR_1 genotype. Chi-square test was used to check for Mendelian distribution (p = 0.9921 and p = 0.0429, respectively). The difference between the total number of wild type (WT) and *Trpv4* knockout (KO) animals was measured using Fisher's exact test (p = 1.00 and p = 0.5175, respectively). **(C)** Difference in total body weight between P21 WT (n = 22) and *Trpv4* KO (n = 21) littermates. The horizontal bars represent the median. (eGFP, enhanced green fluorescent protein)

Microglial characterization in fixed brain slices - Brain surveillance is determined by several factors, among which microglial density in the brain (12). Therefore, we aimed to investigate whether, in the absence of TRPV4, microglial density is lower than the WT model. For this part of the project, we focused on two important brain regions, the motor cortex and the hippocampus. P21 eGFP+ WT and *Trpv4* KO littermates were perfused, and coronal brain slices were prepared for confocal imaging. Density was analyzed in layers 1, 2/3 and 5 of the secondary motor area of the cortex (Fig. 2A). Both WT and *Trpv4* KO littermate mice exhibit a homogenous distribution of microglia throughout the brain, and no significant differences are observed between the groups in all regions (Fig. 2B).

These findings are confirmed by the volumetric density analysis, where we used a higher magnification, showing similar density between both groups (Fig. 3A-B). Similarly, the volumetric density of microglia in the hippocampus was quantified and revealed to be significantly higher than the cortical density (Fig. 3A). *Trpv4* KO mice showed a similar hippocampal density compared to their WT littermates with no significant difference (Fig. 3C). Altogether, our results indicate that *Trpv4*-deficient microglia are homogeneously distributed throughout the brain, and genetic ablation does not alter the number of cells. To further characterize microglial morphology in a

Trpv4-deficient mouse model, we focused on the secondary motor area of the cortex.

Next to branch motility, microglial morphology is also strongly regulated by Ca^{2+}-induced cytoskeletal dynamics (13). Besides, the morphological structure of the cells is a determining factor for microglia when they monitor the brain (12). Therefore, we sought to discern the role of TRPV4 in the structural complexity of the cells using confocal microscopy. Morphological characteristics of microglia were analyzed by examining the process ramifications of the cells using a 3D Sholl analysis. Concentric spheres were applied over the cells every 2 μm from the soma. Microglia derived from WT mice exhibit a highly ramified morphology with first-, second- and third-order branches (Fig. 4A). On the other hand, Sholl analysis revealed that microglia derived from *Trpv4* KO mice display lower intersections of processes with concentric spheres (Fig. 4B) and fewer process endings or tips (Fig. 4C). In addition, in the absence of TRPV4, microglia are less ramified with a significantly lower number of bifurcations (branch points, Fig. 4D) and shorter processes (Fig. 4E-G). Thus, in contrast to density, microglia exhibit a significantly less complex morphology in the constitutive absence of functional TRPV4. These results indicate that TRPV4 acts as a regulator of the morphological structure of microglia, including their process length and formation of process ramifications.
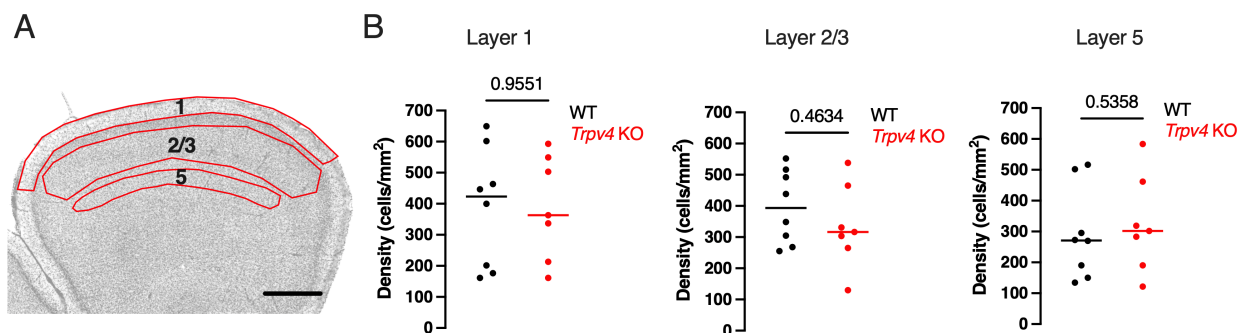
Fig. 2 - Microglial density in the secondary motor area of the cortex in the presence and absence of the TRPV4 channel. (A) Representative confocal image of a perfusion-fixed P21 eGFP+ cortical brain slice. Density was measured in three specific regions, from top to bottom: layer 1, 2/3 and 5. Scale bar, 1 mm. **(B)** Difference in microglial density between wild type (n = 8) and *Trpv4* knockout (n = 7) littermates in the three layers (unpaired, two-tailed Mann-Whitney *U* test). The horizontal bars represent the median. (eGFP, enhanced green fluorescent protein)
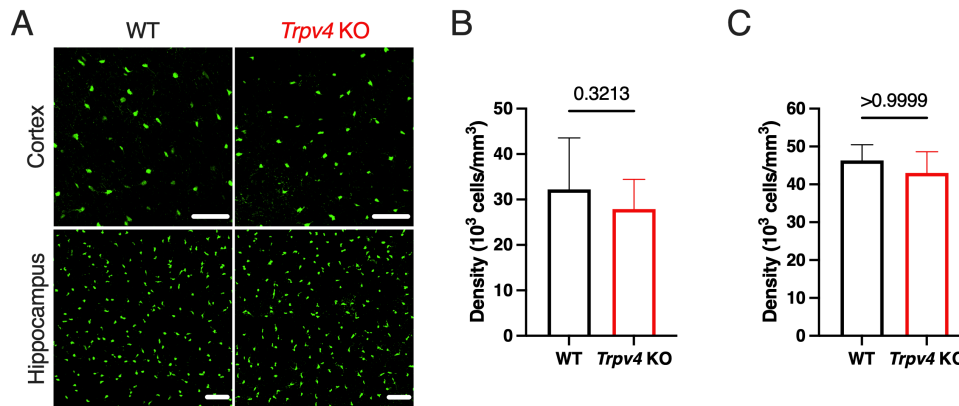
Fig. 3 - Microglial volumetric density in the cortex and hippocampus in the presence and absence of the TRPV4 channel. (A) Representative confocal images of perfusion-fixed P21 eGFP+ wild type (WT) and *Trpv4* knockout (KO) cortical and hippocampal slices imaged with a Z-stack of 20 µm, showing no lower density in the KO slices. Scale bar, 50 µm. **(B)** Difference in microglial density in the cortex between P21 WT (n = 8) and *Trpv4* KO (n = 9) littermates. **(C)** Microglial density in the hippocampus of P21 WT (n = 3) and *Trpv4* KO (n = 3) littermates (unpaired, two-tailed Mann-Whitney *U* test). Bar plots represent the mean with standard deviation. (eGFP, enhanced green fluorescent protein)
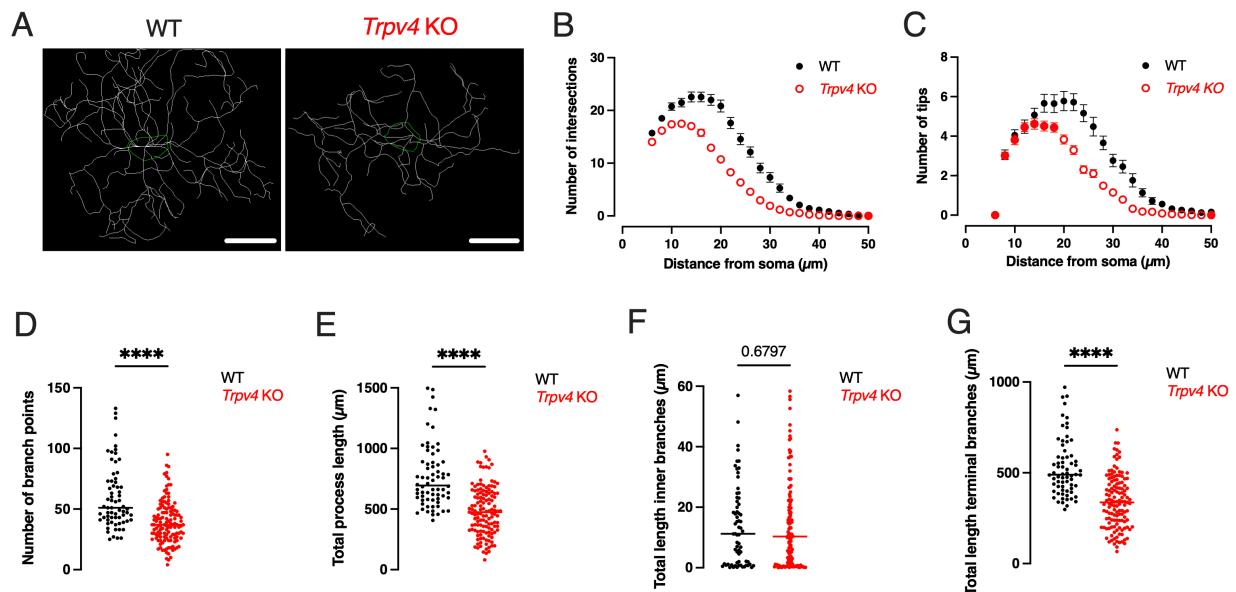

Fig. 4 - Morphological characterization of *Trpv4*-deficient microglia in the cortex. (A) Representative ramified 3D-reconstructions of perfusion-fixed P21 eGFP+ wild type (n = 68) and *Trpv4* knockout (KO) (n = 133) microglia, showing less ramifications in the *Trpv4* KO cell. Scale bar, 10 µm. **(B-G)** Microglial ramification was assessed by Sholl analysis. **(B)** The number of process intersections with shells at distances (in 2 µm increments) from the soma. **(C)** The number of process ending points (tips). Empty data points represent significance ($p < 0.05$; unpaired, multiple Mann-Whitney *U* test). **(D)** The number of bifurcations (branch points). **(E)** Total process length. **(F)** The total length of the inner branches. **(G)** The total length of the terminal branches. **** $p < 0.0001$; unpaired, two-tailed Mann-Whitney *U* test. The horizontal bars represent the median. (eGFP, enhanced green fluorescent protein)

8

Involvement of TRPV4 in microglial branch motility during homeostasis or after acute brain injury - As the key players of the CNS, microglia actively survey the brain area in homeostatic conditions upon stimulation from their environment. It is crucial to detect uncommon signals, such as an injury (ATP) or invading pathogens (8). Besides investigating the effect of TRPV4 on surveillance through its contribution to the morphology of microglia, we were interested in whether channel activity is essential to regulate branch motility. We investigated the role of TRPV4 in microglial process movements using acute cortical brain slices from P21 eGFP+ WT and *Trpv4* KO littermates for *ex vivo* imaging with two-photon microscopy. A selected group of slices derived from WT mice was incubated with the TRPV4 antagonist GSK21 to induce acute TRPV4 inhibition. GSK21 is a chemical compound that binds to the channel's transmembrane domain and blocks conductance hence inhibiting Ca^{2+} influx (48). In homeostatic conditions, microglia derived from WT mice exhibit a dynamic movement of their branches, surveying the neighboring environment (Fig. 5A). In the absence or inhibition of TRPV4, microglia cover significantly less brain area after 10 min of surveillance than WT cells, as displayed in Fig. 5B-C. Both conditions are associated with less process motility, hence a lower rate of surveillance. Therefore, TRPV4 might act as a significant contributor in the process of microglial surveillance. Whether the channel shows similar functions during microglial activation has to be investigated.

When microglia detect uncommon changes in the brain during surveillance, the cells become activated and display directed motility towards the injury (10). This event is highly dependent on $_i[Ca^{2+}]$ to stimulate the turnover of the actin cytoskeleton for an outward movement of processes towards the lesion (13, 23). We were interested in discerning the role of TRPV4 in the process of directed branch motility after microglial activation. A laser-induced brain injury was evoked on WT, *Trpv4* KO and GSK21-incubated acute cortical brain slices for *ex vivo* imaging with two-photon microscopy (Fig. 6A). This way, we mimic brain damage associated with cell death and an abundant release of chemical cues like ATP (10). These signals will activate purinergic receptors (10), allowing us to study directed motility resulting

from these receptors without the contribution of the mechanosensitive TRPV4 channel. We quantified the average speed of extending processes per cell and the instantaneous speed of processes over time.
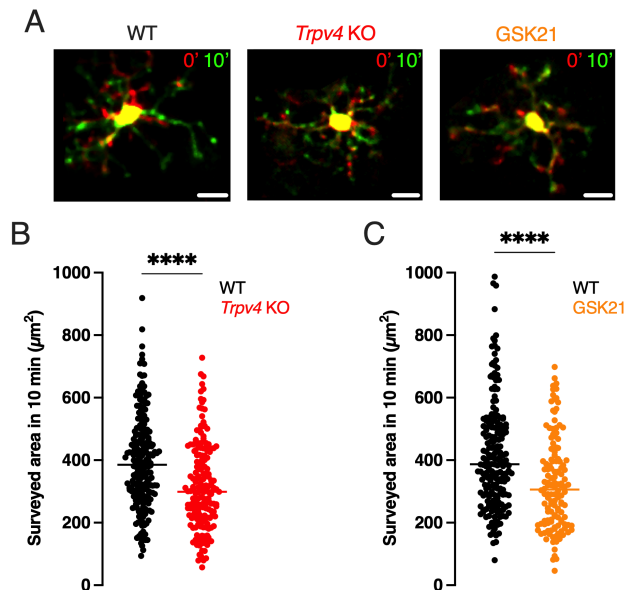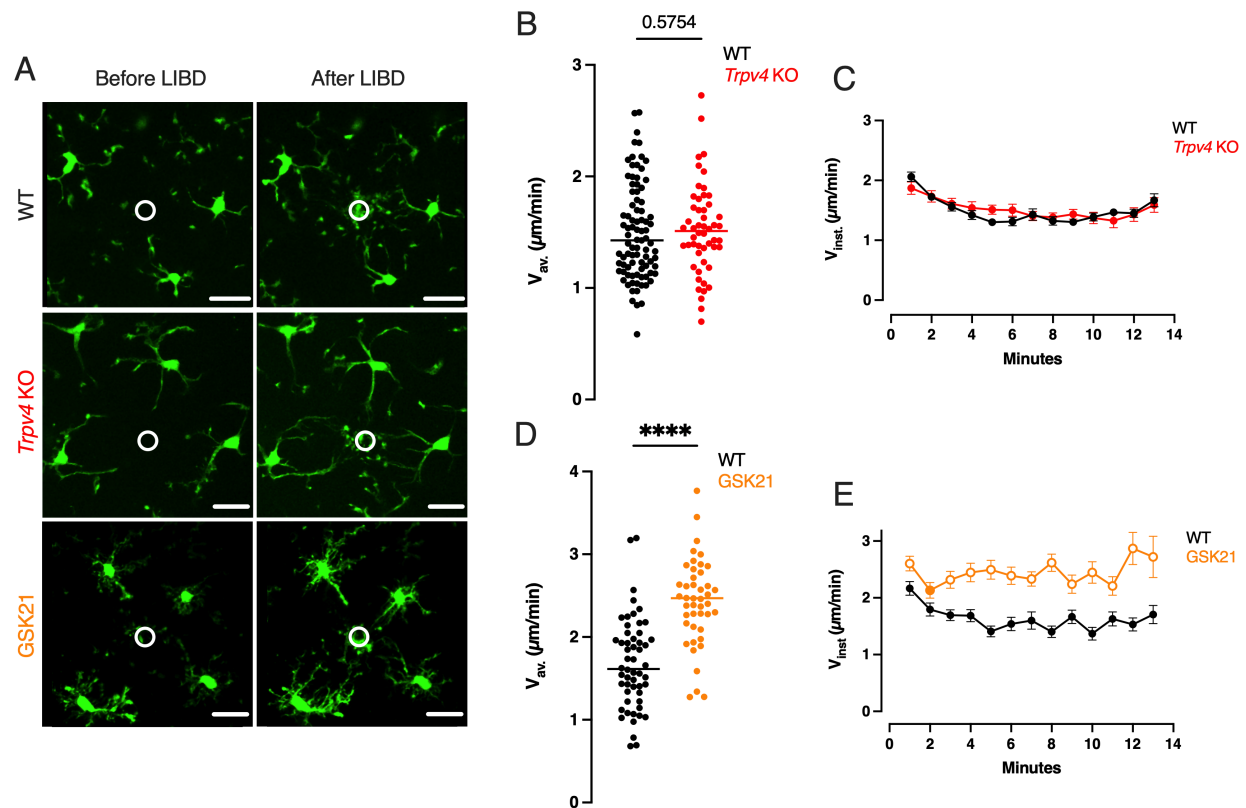

Fig. 5 - Changes in microglial surveillance due to a lack of TRPV4. (A) Representative two-photon time-lapse images of acute P21 eGFP+ untreated wild type (WT) and *Trpv4* knockout (KO) cortical slices and slices treated with the TRPV4 antagonist (GSK2193874 (GSK21), 10 μM) after 0 min (red) and 10 min (green). Scale bar, 10 μm. **(B-C)** Quantification of the surveyed brain area after 10 min. **(B)** Difference in microglial surveillance between WT (n = 211) and *Trpv4* KO (n = 179) cells. **(C)** Difference in surveillance between untreated (WT) (n = 198) and inhibitor-treated (GSK21) (n = 136) microglia. **** p < 0.0001; unpaired, two-tailed Mann-Whitney *U* test. The horizontal bars represent the median. (eGFP, enhanced green fluorescent protein)

The instantaneous speeds represent the average process speed per cell per time frame of 1 min. After the injury, all surrounding microglia extend their processes towards the lesion site within minutes in the WT condition with a similar response in the KO and GSK21-treated conditions (Fig. 6A). The average speed of extending processes is not lower in the absence of TRPV4, indicating that a genetic modification does not hinder directed motility (Fig. 6B-C). In contrast, after acute inhibition of TRPV4, both the average

and the instantaneous speed of extending processes are significantly increased compared to the untreated WT cells (Fig. 6D-E). Results indicate that the mechanisms behind directed motility are likely not dependent on TRPV4 channel activity and rely on other receptors.

The role of TRPV4 in phagocytic activity in vitro - Besides morphology and branch motility, we investigated the role of TRPV4 in microglial phagocytosis, an important event after brain injury (13). Mechanical stimuli from the injury site might trigger TRPV4 activity, and microglia will transform into phagocytic cells to take up cellular debris and clear the area to restore homeostasis. Since this process involves cytoskeletal

rearrangements, we were interested in whether TRPV4 provides fuel for this machinery via $_i[Ca^{2+}]$ increase. Microglia, isolated from P21 WT and *Trpv4* KO littermates, were cultured in optimized media to obtain a ramified morphology. To mimic phagocytosis *in vitro*, the cells were incubated with neuron-derived synaptosomes from adult mice and fixed for confocal imaging. Additionally, a selected group of WT cells was treated with two different GSK21 concentrations for acute inhibition of TRPV4. We demonstrate that after 1 h of incubation with synaptosomes, WT cells contain synaptosomes within their soma, showing the phagocytic process has happened (Fig. 7A). In the

Fig. 6 - Changes in microglial directed motility towards damaged brain areas due to a lack of TRPV4. **(A)** Representative two-photon time-lapse images of acute P21 eGFP+ untreated wild type (WT) and *Trpv4* knockout (KO) cortical slices and slices treated with the TRPV4 antagonist (GSK2193874 (GSK21), 10 μM) before and after laser-induced brain damage (LIBD, indicated by the white circle). Scale bar, 20 μm. **(B-C)** Quantification of directed motility of WT (n = 89) and *Trpv4* KO (n = 52) cortical microglia. **(B)** The average speed of extending processes per cell towards the injury. **(C)** Instantaneous process speed per cell per time frame of 1 min. **(D-E)** Quantification of directed motility of untreated (WT) (n = 54) and inhibitor-treated (GSK21) (n = 46) cortical microglia, information idem to B-C. **** p < 0.0001; unpaired, two-tailed Mann-Whitney *U* test. Empty data points represent significance (p < 0.05; unpaired, multiple Mann-Whitney *U* test). The horizontal bars represent the median. (eGFP, enhanced green fluorescent protein)

absence of TRPV4, phagocytic activity is significantly lower in microglia, with less percentage of the cell area covered by synaptosomes (Fig. 7B). In contrast to this, both concentrations of the pharmacological compound induced increased phagocytosis of synaptosomes compared to the WT cells. *Trpv4*-deficient microglia show a lower uptake of cellular debris, suggesting the importance of TRPV4 as a Ca^{2+} channel to induce cytoskeletal dynamics hence phagocytosis.

A
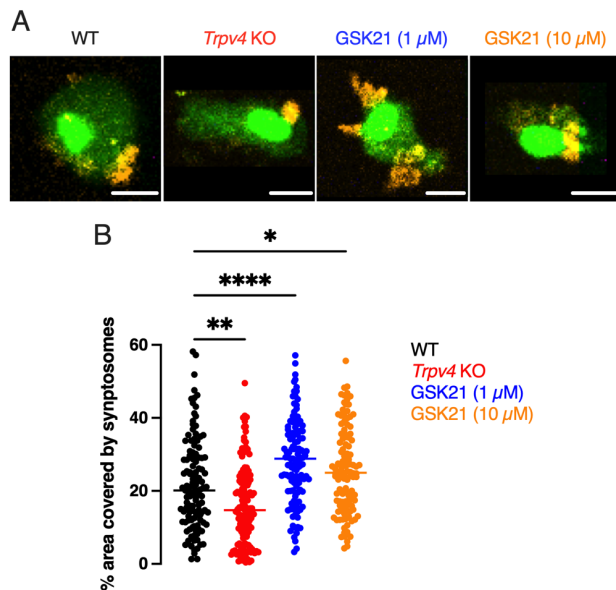
Fig. 7 - Effect of TRPV4 receptor knockout or inhibition on microglial phagocytosis *in vitro*. (A) Representative confocal images of P21 eGFP+ isolated microglia from WT and *Trpv4* KO mice and cells treated with the acute TRPV4 inhibitor (GSK2193874 (GSK21), 1 µM and 10 µM) incubated with DiI-labeled synaptosomes for 1 h. Scale bar, 10 µm. **(B)** Percentage of the cell area covered by synaptosomes after 1 h. * $p < 0.05$, ** $p < 0.01$ and **** $p < 0.0001$; unpaired, Dunn's multiple comparison test. The horizontal bars represent the median. (eGFP, enhanced green fluorescent protein)

DISCUSSION

Microglia are resident immune cells of the CNS and are crucial during brain development and throughout life to maintain homeostasis (1). Microglial dysfunction is associated with several life-altering developmental brain disorders highlighting the indispensable role of the cells (3).

Therefore, it is crucial to understand their complexity and the underlying mechanisms of microglial functioning. It is known that microglia require motility of their processes to survey the brain and anticipate when the balance in the brain is disturbed to clear the area using phagocytosis (12). In this project, we investigated the role of the mechanosensory TRPV4 channel in these microglial functions.

To characterize microglia in the presence and absence of TRPV4, we used WT and *Trpv4* KO mouse littermates. TRPV4 is involved in a myriad of critical cellular processes. However, genetic ablation is only associated with minor phenotypes such as hearing problems, defective stretch sensation in the bladder wall, pain and pressure sensory impairments and thicker bones (49). We found that our breedings using *Trpv4* heterozygous couples provide equal numbers of WT and *Trpv4* KO pups with normal phenotypic development and no differences in total body weight. In addition, the *Trpv4* KO phenotype is not associated with changes in microglial density in the cortex and hippocampus, which is a contributing factor to microglial functioning (12). The cells are also similarly distributed in WT and *Trpv4* KO animals with a higher density in the hippocampus than in the cortex, as described in the literature (44). With these results, we demonstrate that *Trpv4*-deficient mice exhibit normal embryonic and postnatal development with a homogenous microglial distribution throughout the brain.

Although the lack of TRPV4 does not hinder microglial distribution within the brain, it does affect the morphological complexity of the cells. Microglia in the healthy brain are highly ramified, which is intracellularly regulated by the structure of their cytoskeleton (10, 13). In the absence of TRPV4, microglia are less ramified with shorter branches and fewer bifurcations. These findings are in line with recent findings by others showing that 1) the microglial architecture (e.g. ramifications) is dependent on TRPV4 activity in response to osmotic stress *in vitro* (41) and 2) genetic deficiency of *Trpv4* is associated with a lower total process length and fewer processes per cell than their WT littermates upon heat stimulation (28). The morphological changes of microglia probably affect the total volume of the cells, although further research is required to elucidate this. A lower cellular volume implies that less space is covered

by the cells in the brain, resulting in wider unsupervised areas. These phenotypic characteristics might alter or affect microglial functioning in the brain, such as surveillance, considering that the cells rely on their processes to carry out their functions.

This was confirmed by our experiments, where we show that genetic ablation of *Trpv4* is associated with a lower surveyed area by microglia in the brain. The insufficient surveillance of the brain is due to the phenotypical changes of the *Trpv4*-deficient microglia, preventing them from scanning more area. However, acute inhibition of TRPV4 also induces a reduction in surveillance compared to the WT condition. The difference between the *Trpv4* KO and acute TRPV4-inhibited model is that *Trpv4* KO microglia are genetically modified, which correlates with fewer ramifications. Inhibitor-treated cells are derived from WT mice and are therefore highly ramified. Consequently, next to microglial morphology, other TRPV4-regulated underlying mechanisms are involved in surveillance. Stas *et al.* demonstrated that the absence or inhibition of TRPV4 is associated with lower tubulin dynamics in microglia (50). Furthermore, inhibitor-treated microglia showed less and shorter filopodia, which are actin enriched structures, with more downward movement or dynamics (50). This probably leads to a decreased motility of microglial branches and a lower capacity to scan the brain area, hence less surveillance. Nashimoto *et al.* investigated whether TRPV4 mediates microglial branch motility through thermosensation and proved that a lack of TRPV4 impairs process motility *in vivo*, further confirming our observations (28). However, whether next to motility, the speed of moving branches is affected is still under investigation. In conclusion, TRPV4 is crucial for optimal branch motility during surveillance. The channel's activity induces cytoskeletal dynamics through a Ca^{2+}-regulated pathway or direct via the interaction of TRPV4 with tubulin and actin through its C-terminus (42).

Since microglia receive mechanical stimuli of the ECM through their ß1 integrin receptors, and TRPV4 is activated by shear, mechanical and osmotic stress (3, 41), we suggest that the process of branch motility is initiated by mechanosensation where the ECM-integrin interaction activates TRPV4. Previous research demonstrated that

TRPV4 is a mechanosensor for matrix stiffness, cell stretching and mechanical forces applied to ß1 integrins in chondrocytes (35). Likewise, ß1 integrin stimulation in endothelial cells is transferred through the cytoskeletal elements triggering ultra-rapid TRPV4 activity. The resulting Ca^{2+} signal triggers cytoskeletal rearrangements and thereby cellular motility and morphological changes (26). Furthermore, Ca^{2+} influx through TRPV4 in response to integrins stimulates motility of endothelial cells by downstream reactivation of ß1 integrins (51). This last mechanism suggests a third possible pathway of TRPV4-induced branch motility, next to $_i[Ca^{2+}]$ and the TRPV4-cytoskeleton interaction.

Microglial surveillance is a multicomponent event where the cells interact with surrounding cells such as astrocytes and neurons. Next to microglia, these cells also express TRPV4 on their plasma membrane (37, 42). Therefore, the effect of *Trpv4* deficiency on surveillance might be a combined effect because of the channel's role in different cell types of the microglial environment, including microglia themselves. Umpierre *et al.* showed that neuronal activity modulates microglial branch motility and Ca^{2+} signaling (18). An alternative approach to overcome these environmental effects is to create a bone marrow chimera with a microglia-specific *Trpv4* deficiency. It allows the study of specific effects of microglial TRPV4 on microglial functioning.

In addition to monitoring the healthy brain, microglia play a protective role and respond to any uncommon change in the environment by extending their processes and transforming into an activated phenotype to restore balance (10). Although this event is strongly Ca^{2+}-regulated, TRPV4 seems not to be a key player in directed motility as the speed of extending processes towards the lesion is similar between WT and *Trpv4* KO microglia. Acute brain damage is associated with a strong ATP release, a major stimulus for directed motility (10). This results in activating ATP-sensitive channels like purinergic receptors, provoking a high increase of $_i[Ca^{2+}]$ to induce branch motility (18). The abundant ATP signal can overrule TRPV4 capacities or decrease the channel's sensitivity reducing its contribution to this event. On the other hand, the ATP-mediated, extremely fast, directed motility might mechanically stimulate TRPV4 to an extreme degree, thereby reversing its activity to

downregulate the extent of process motility and the Ca^{2+} signal. Thus, the channel might contribute to a negative feedback loop to control the extension rate of processes. In the absence of TRPV4, this control function might be taken over by compensatory mechanisms like an increased contribution of other TRP channels. We could investigate an increased expression of Ca^{2+} channels in *Trpv4* KO cells via single-cell RNA sequencing. These channels might decrease microglial response to a similar level compared to the WT cells. After acute inhibition with pharmacological tools, compensatory mechanisms are less likely to operate. Therefore, functional impairment of TRPV4 will hinder this control function, leading to a robust response after injury. These implications might expose the redundant role of TRPV4 in the process of directed motility.

Microglia are the primary phagocytes of the brain (52). Directed motility after brain injury is followed by further cell activation and transformation to phagocytic cells (13). The plasma membrane deforms together with cytoskeletal rearrangements to allow the engulfment of particles (52). TRPV4 plays a crucial role in determining phagocytic capacity in microglia. Phagocytosis in response to mechanical stimuli occurs through a ß1 integrin-dependent mechanism (53), indicating the involvement of the ECM-integrin-TRPV4 axis as previously described. In contrast, in the absence of functional TRPV4 channels, phagocytic activity strongly increases. GSK21 treatment affects microglial morphology *in vitro* by reducing circularity (e.g. ramifications) and area of the cells (50). This will increase the ratio of the phagocytosed cargo within the cell to the cellular area, increasing the area covered with particles and therefore showing an artificial increase in uptake.

In conclusion, this study shows that (a) WT and *Trpv4* KO mice develop equally with similar total body weight and a similar microglial density in the brain, (b) A TRPV4 receptor KO affects the morphological structure of microglia with fewer ramifications, (c) TRPV4 channel activity contributes to microglial branch motility during brain surveillance, while its role during directed motility is redundant and (d) Phagocytic activity of microglia decreases in the constitutive absence of functional TRPV4. With these interesting findings, we demonstrate that TRPV4 regulates several microglial functions and contributes to the optimal functioning of the cells. It provides new insight into the underlying mechanisms of microglia. To further explore TRPV4 in microglia, we can study the mechanism of TRPV4 activation in microglia and whether this is through mechanosensation. For example, by using hydrogels, we can investigate whether microglia exhibit mechanical-dependent motility *in vitro*. Additionally, we can demonstrate the TRPV4-ß1 integrin interaction in microglia and explore the primary mechanism of how TRPV4 interacts with the cytoskeleton to stimulate motility. As mentioned above, using single-cell RNA sequencing, we can reveal possible compensatory mechanisms of TRPV4. Another significant added value to our study would be conducting *in vivo* experiments on *Trpv4* KO animals to discern the effect of a genetic modification on cognition and behavior or to strengthen our current data with *in vivo* transcranial imaging using two-photon microscopy.

CONCLUSION

In this project, we explore the role of TRPV4 in microglia. Mechanosensory channels have not been extensively described in microglia, and therefore, we identify new mechanisms and processes for a better characterization of microglia in health and disease. This way, we provide new insight to understand microglial regulation and functioning. This can be highly instrumental in developing therapeutic strategies for microglia-related diseases or other CNS pathologies.

REFERENCES

1.   Wolf SA, Boddeke HW, Kettenmann H. Microglia in Physiology and Disease. Annu Rev Physiol. 2017;79:619-43.

2.   Sominsky L, De Luca S, Spencer SJ. Microglia: Key players in neurodevelopment and neuronal plasticity. Int J Biochem Cell Biol. 2018;94:56-60.

3.   Smolders SM, Kessels S, Vangansewinkel T, Rigo JM, Legendre P, Brone B. Microglia: Brain cells on the move. Prog Neurobiol. 2019;178:101612.

4.   Colonna M, Butovsky O. Microglia Function in the Central Nervous System During Health and Neurodegeneration. Annu Rev Immunol. 2017;35:441-68.

5.   Eyo UB, Mo M, Yi MH, Murugan M, Liu J, Yarlagadda R, et al. P2Y12R-Dependent Translocation Mechanisms Gate the Changing Microglial Landscape. Cell Rep. 2018;23(4):959-66.

6.   Ohsawa K, Irino Y, Sanagi T, Nakamura Y, Suzuki E, Inoue K, et al. P2Y12 receptor-mediated integrin-beta1 activation regulates microglial process extension induced by ATP. Glia. 2010;58(7):790-801.

7.   Prata J, Santos SG, Almeida MI, Coelho R, Barbosa MA. Bridging Autism Spectrum Disorders and Schizophrenia through inflammation and biomarkers - pre-clinical and clinical investigations. J Neuroinflammation. 2017;14(1):179.

8.   Madry C, Kyrargyri V, Arancibia-Carcamo IL, Jolivet R, Kohsaka S, Bryan RM, et al. Microglial Ramification, Surveillance, and Interleukin-1beta Release Are Regulated by the Two-Pore Domain K(+) Channel THIK-1. Neuron. 2018;97(2):299-312 e6.

9.   Mizoguchi Y, Kato TA, Horikawa H, Monji A. Microglial intracellular Ca(2+) signaling as a target of antipsychotic actions for the treatment of schizophrenia. Front Cell Neurosci. 2014;8:370.

10.   Davalos D, Grutzendler J, Yang G, Kim JV, Zuo Y, Jung S, et al. ATP mediates rapid microglial response to local brain injury in vivo. Nat Neurosci. 2005;8(6):752-8.

11.   Farber K, Kettenmann H. Purinergic signaling and microglia. Pflugers Arch. 2006;452(5):615-21.

12.   Madry C, Attwell D. Receptors, ion channels, and signaling mechanisms underlying microglial dynamics. J Biol Chem. 2015;290(20):12443-50.

13.   Franco-Bocanegra DK, McAuley C, Nicoll JAR, Boche D. Molecular Mechanisms of Microglial Motility: Changes in Ageing and Alzheimer's Disease. Cells. 2019;8(6).

14.   Kyrargyri V, Madry C, Rifat A, Arancibia-Carcamo IL, Jones SP, Chan VTT, et al. P2Y13 receptors regulate microglial morphology, surveillance, and resting levels of interleukin 1beta release. Glia. 2020;68(2):328-44.

15.   Nimmerjahn A, Kirchhoff F, Helmchen F. Resting microglial cells are highly dynamic surveillants of brain parenchyma in vivo. Science. 2005;308(5726):1314-8.

16.   Pozner A, Xu B, Palumbos S, Gee JM, Tvrdik P, Capecchi MR. Intracellular calcium dynamics in cortical microglia responding to focal laser injury in the PC::G5-tdT reporter mouse. Front Mol Neurosci. 2015;8:12.

17.   Nayak D, Roth TL, McGavern DB. Microglia development and function. Annu Rev Immunol. 2014;32:367-402.

18.   Umpierre AD, Bystrom LL, Ying Y, Liu YU, Worrell G, Wu LJ. Microglial calcium signaling is attuned to neuronal activity in awake mice. Elife. 2020;9.

19.   Haynes SE, Hollopeter G, Yang G, Kurpius D, Dailey ME, Gan WB, et al. The P2Y12 receptor regulates microglial activation by extracellular nucleotides. Nat Neurosci. 2006;9(12):1512-9.

20.   Kettenmann H, Hanisch UK, Noda M, Verkhratsky A. Physiology of microglia. Physiol Rev. 2011;91(2):461-553.

21.   Konno M, Shirakawa H, Iida S, Sakimoto S, Matsutani I, Miyake T, et al. Stimulation of transient receptor potential vanilloid 4 channel suppresses abnormal activation of microglia induced by lipopolysaccharide. Glia. 2012;60(5):761-70.

22.   Farber K, Kettenmann H. Functional role of calcium signals for microglial function. Glia. 2006;54(7):656-65.

23.   Mizoguchi Y, Monji A. Microglial Intracellular Ca(2+) Signaling in Synaptic Development and its Alterations in Neurodevelopmental Disorders. Front Cell Neurosci. 2017;11:69.

14

24.   Kaazempur Mofrad MR, Abdul-Rahim NA, Karcher H, Mack PJ, Yap B, Kamm RD. Exploring the molecular basis for mechanosensation, signal transduction, and cytoskeletal remodeling. Acta Biomater. 2005;1(3):281-93.

25.   Huttenlocher A, Horwitz AR. Integrins in cell migration. Cold Spring Harb Perspect Biol. 2011;3(9):a005074.

26.   Matthews BD, Thodeti CK, Tytell JD, Mammoto A, Overby DR, Ingber DE. Ultra-rapid activation of TRPV4 ion channels by mechanical forces applied to cell surface beta1 integrins. Integr Biol (Camb). 2010;2(9):435-42.

27.   Echeverry S, Rodriguez MJ, Torres YP. Transient Receptor Potential Channels in Microglia: Roles in Physiology and Disease. Neurotox Res. 2016;30(3):467-78.

28.   Nishimoto R, Derouiche S, Eto K, Deveci A, Kashio M, Kimori Y, et al. Thermosensitive TRPV4 channels mediate temperature-dependent microglia movement. Proc Natl Acad Sci U S A. 2021;118(17).

29.   Jiang X, Newell EW, Schlichter LC. Regulation of a TRPM7-like current in rat brain microglia. J Biol Chem. 2003;278(44):42867-76.

30.   Kraft R, Grimm C, Grosse K, Hoffmann A, Sauerbruch S, Kettenmann H, et al. Hydrogen peroxide and ADP-ribose induce TRPM2-mediated calcium influx and cation currents in microglia. Am J Physiol Cell Physiol. 2004;286(1):C129-37.

31.   Beck A, Penner R, Fleig A. Lipopolysaccharide-induced down-regulation of Ca2+ release-activated Ca2+ currents (I CRAC) but not Ca2+-activated TRPM4-like currents (I CAN) in cultured mouse microglial cells. J Physiol. 2008;586(2):427-39.

32.   Miyake T, Shirakawa H, Nakagawa T, Kaneko S. Activation of mitochondrial transient receptor potential vanilloid 1 channel contributes to microglial migration. Glia. 2015;63(10):1870-82.

33.   Hassan S, Eldeeb K, Millns PJ, Bennett AJ, Alexander SP, Kendall DA. Cannabidiol enhances microglial phagocytosis via transient receptor potential (TRP) channel activation. Br J Pharmacol. 2014;171(9):2426-39.

34.   Everaerts W, Nilius B, Owsianik G. The vanilloid transient receptor potential channel TRPV4: from structure to disease. Prog Biophys Mol Biol. 2010;103(1):2-17.

35.   Sharma S, Goswami R, Zhang DX, Rahaman SO. TRPV4 regulates matrix stiffness and TGFbeta1-induced epithelial-mesenchymal transition. J Cell Mol Med. 2019;23(2):761-74.

36.   Liedtke W, Tobin DM, Bargmann CI, Friedman JM. Mammalian TRPV4 (VR-OAC) directs behavioral responses to osmotic and mechanical stimuli in Caenorhabditis elegans. Proc Natl Acad Sci U S A. 2003;100 Suppl 2:14531-6.

37.   Kanju P, Liedtke W. Pleiotropic function of TRPV4 ion channels in the central nervous system. Exp Physiol. 2016;101(12):1472-6.

38.   Becker D, Muller M, Leuner K, Jendrach M. The C-terminal domain of TRPV4 is essential for plasma membrane localization. Mol Membr Biol. 2008;25(2):139-51.

39.   Nilius B, Flockerzi V. Mammalian transient receptor potential (TRP) cation channels. Preface. Handb Exp Pharmacol. 2014;223:v - vi.

40.   Wang Z, Zhou L, An D, Xu W, Wu C, Sha S, et al. TRPV4-induced inflammatory response is involved in neuronal death in pilocarpine model of temporal lobe epilepsy in mice. Cell Death Dis. 2019;10(6):386.

41.   Redmon SN, Yarishkin O, Lakk M, Jo A, Mustafic E, Tvrdik P, et al. TRPV4 channels mediate the mechanoresponse in retinal microglia. Glia. 2021;69(6):1563-82.

42.   Goswami C, Kuhn J, Heppenstall PA, Hucho T. Importance of non-selective cation channel TRPV4 interaction with cytoskeleton and their reciprocal regulations in cultured cells. PLoS One. 2010;5(7):e11654.

43.   Shi M, Du F, Liu Y, Li L, Cai J, Zhang GF, et al. Glial cell-expressed mechanosensitive channel TRPV4 mediates infrasound-induced neuronal impairment. Acta Neuropathol. 2013;126(5):725-39.

44.   Tan YL, Yuan Y, Tian L. Microglial regional heterogeneity and its role in the brain. Mol Psychiatry. 2020;25(2):351-67.

45.   Schindelin J, Arganda-Carreras I, Frise E, Kaynig V, Longair M, Pietzsch T, et al. Fiji: an open-source platform for biological-image analysis. Nat Methods. 2012;9(7):676-82.

46.   Peng H, Ruan Z, Long F, Simpson JH, Myers EW. V3D enables real-time 3D visualization and quantitative analysis of large-scale biological image data sets. Nat Biotechnol. 2010;28(4):348-53.

47.   Bohlen CJ, Bennett FC, Bennett ML. Isolation and Culture of Microglia. Curr Protoc Immunol. 2019;125(1):e70.

48.   Cheung M, Bao W, Behm DJ, Brooks CA, Bury MJ, Dowdell SE, et al. Discovery of GSK2193874: An Orally Active, Potent, and Selective Blocker of Transient Receptor Potential Vanilloid 4. ACS Med Chem Lett. 2017;8(5):549-54.

49.   Grace MS, Bonvini SJ, Belvisi MG, McIntyre P. Modulation of the TRPV4 ion channel as a therapeutic target for disease. Pharmacol Ther. 2017;177:9-22.

50.   Stas N BJ, Brône B, Alpizar YA. Transient Receptor Potential Vanilloid 4 inhibition reduces microglial cytoskeleton dynamics *in vitro*. Master thesis manuscript. 2021.

51.   Thodeti CK, Matthews B, Ravi A, Mammoto A, Ghosh K, Bracha AL, et al. TRPV4 channels mediate cyclic strain-induced endothelial cell reorientation through integrin-to-integrin signaling. Circ Res. 2009;104(9):1123-30.

52.   Koenigsknecht J, Landreth G. Microglial phagocytosis of fibrillar beta-amyloid through a beta1 integrin-dependent mechanism. J Neurosci. 2004;24(44):9838-46.

53.   Bhalla S, Shiratsuchi H, Craig DH, Basson MD. beta(1)-integrin mediates pressure-stimulated phagocytosis. Am J Surg. 2009;198(5):611-6.